Table PS-1. Collective dose from routine transport for the truck route from Maine Yankee Nuclear Power Plant to Oak Ridge National Lab (person-Sv)

Exposed Population	Rural	Suburban	Urban	Urban Rush Hour	Total
Residents near route	7.9×10^{-6}	1.4×10^{-4}	2.9×10^{-6}	6.5×10^{-8}	1.5×10^{-4}
Traffic on the route	1.3×10^{-4}	2.3×10^{-4}	5.4×10^{-5}	5.0×10^{-6}	4.2×10^{-4}
Residents near truck stops	1.1×10^{-6}	2.3×10^{-5}	*	*	2.4×10^{-5}
Truck Crew	5.6×10^{-8}		4.8×10^{-9}		6.1×10^{-8}
Escort	4.7×10^{-8}		4.3×10^{-9}		5.1×10^{-8}
Inspectors (10 inspections)					3.2×10^{-8}
Truck stop workers					2.0×10^{-9}
Background					8.81

*Most truck stops are located in rural or suburban areas

The collective doses calculated for routine transportation have gone down with each successive study of the risks from spent fuel transportation. Figure PS-2 shows a comparison of the collective doses calculated in the three studies for truck transportation.

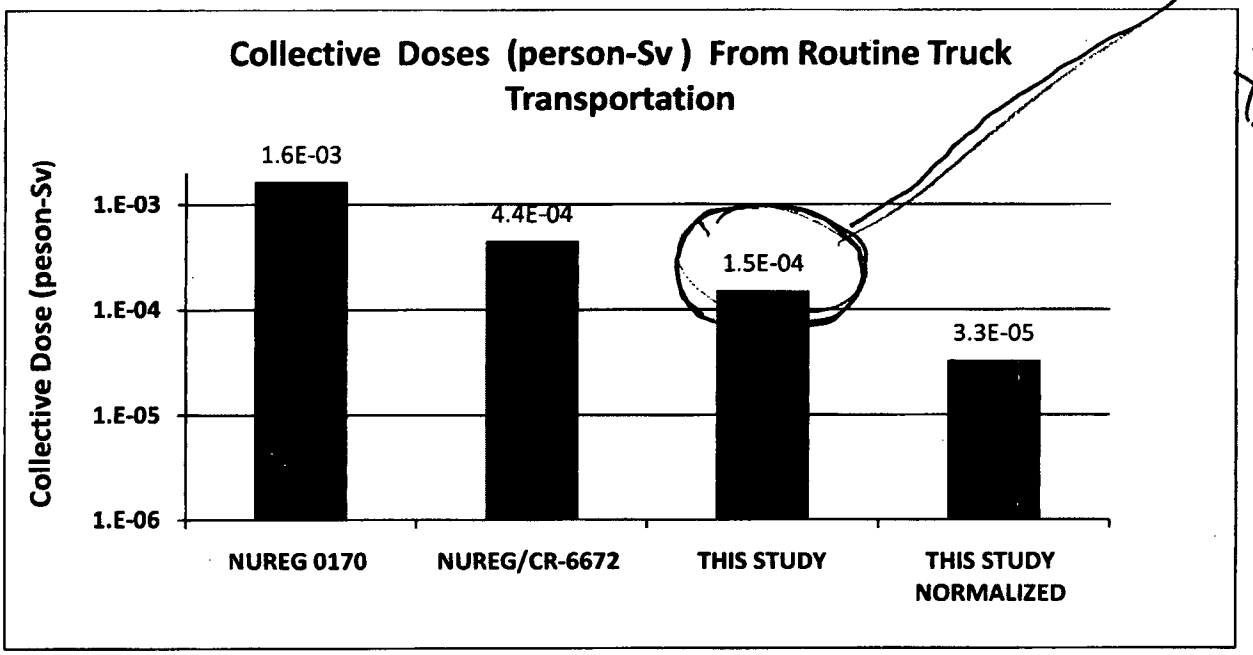

Figure PS-2. Collective doses (person-Sv) from routine truck transportation

The study uses current (2006 to 2008) truck and rail accident statistics to determine the probability of an accident and the severity of that accident. Detailed analyses are performed to evaluate how the cask responds to the accident. Figure PS-3 shows one impact scenario, a 97 kph (60 mph) corner impact onto a rigid target, and the resulting deformations. Almost all of the deformation is in the impact limiter, a device that is added to the cask to absorb energy, much

neglected in the prior studies, the dose that results from accidents where there is no release and no loss of shielding, but increased exposure to a cask that is stopped for an extended period of time. Considering this scenario is important because over 99.999 percent of all accident scenarios do not lead to release or loss of shielding.

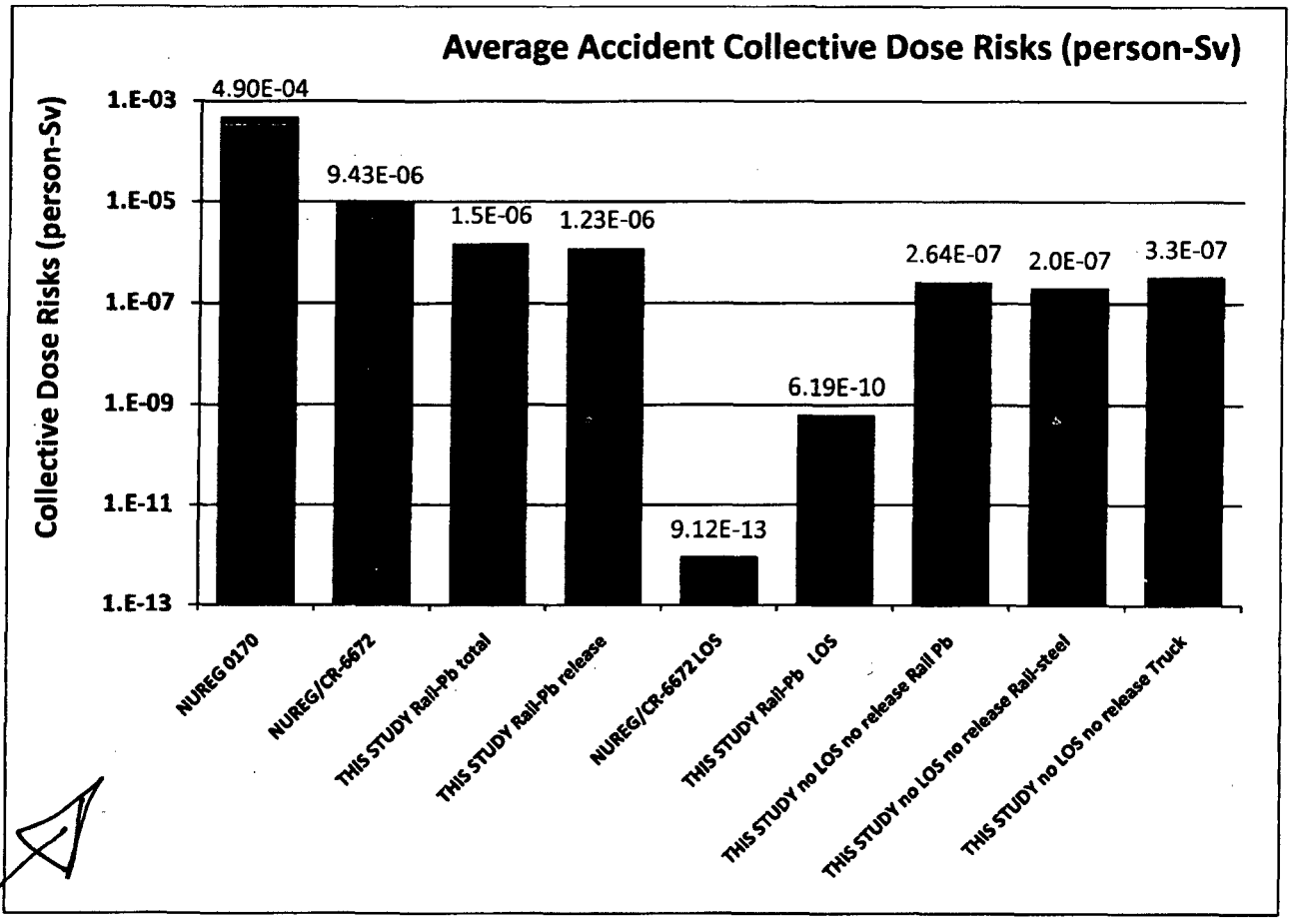

Figure PS-5. Accident collective dose risks

One other point of comparison between the studies is the maximum consequence of an accident. For NUREG-0170 this was about 110 person-Sv, for NUREG/CR-6672 it was about 9000 person-Sv, and for this study it is about 2 person-Sv. Not only is the estimated risk of spent fuel transportation exceedingly small, but the estimated maximum consequence is also very small.

The Public Will never understand this!

cask damage was considerably less than NUREG-0170 had estimated. Although the Modal Study was not a risk analysis, since it did not consider the radiological consequence of accidents, risks less than those estimated in NUREG-0170 could be inferred.

NUREG/CR-6672 built on the Modal Study by refining the mechanical stress/thermal stress matrix and recasting it as a matrix of impact speed and temperature. In addition, NUREG/CR-6672 developed expressions for the behavior of spent fuel in accidents and potential release of this material and analyzed the potential releases. The enhanced modeling capability available for NUREG/CR-6672 allowed analysis of the detailed structural and thermal damage to transportation casks. NUREG/CR-6672 also used results of experiments by Lorenz (1980), Sandoval, et al (1988), and Sanders, et al (1992) to estimate releases of radioactive material from the fuel rods to the cask interior and from the cask interior to the environment following very severe accidents. The radionuclides available for release in the accidents studied in NUREG/CR-6672 are from relatively low burnup (30 GWD/MTU) and relatively high burnup (60 GWD/MTU) PWR and BWR fuel, although the transportability of the high burnup fuel was not considered. The particular characteristics of high-burnup fuel shown by Einziger (2007) and Einziger and Beyer (2007) were investigated after the publication of NUREG/CR-6672 and could not have been included in the NUREG/CR-6672 analysis. NUREG/CR-6672 studied the behavior of two generic truck casks and two generic rail casks which were each composites of several certified casks.

The results of the NUREG/CR-6672 risk assessment were several orders of magnitude less than the estimates of NURE 0170, and concluded that no radioactive material would be released in more than 99.99 percent of accidents involving spent fuel. These low risk estimates resulted from the use of refined and improved analytical and modeling techniques, exemplified by the finite element analyses of cask structure, and limited experimental data.

The present study analyzed the behavior of three currently certified casks carrying Westinghouse 17x17 pressurized water reactor (PWR) fuel with 45,000 megawatt-days per metric ton of uranium (MWD/MTU) burnup, the highest burnup that any of the three casks are certified to carry. The resulting radiological risks are less than those reported in NUREG/CR-6672. For routine transportation, the risks are slightly less than those estimated in NUREG/CR-6672, because the actual external dose rates are less than the regulatory maximum used in the other studies, and because of code and modeling improvement. For accidents, the radiological risks calculated in the current study are at least an order of magnitude less. The improvement of the risk estimates of NURGE-0170 and NUREG/CR-6672 is the result of new data and observations, and improved modeling techniques.

1.2 Risk

Risk provides understanding of events that might happen in the future. It is always a projection. Once an event happens, it is no longer a risk. Because risks are projections of potential future events, calculations of risk are based on estimates and approximations.

Understanding transportation risk is integral to understanding the environmental and related human health impact of radioactive materials transportation. A large amount of data exists for deaths, injuries, and damage from traffic accidents, but there are no data on health effects caused

CHAPTER 3

CASK RESPONSE TO IMPACT ACCIDENTS

3.1 Introduction

Spent fuel casks are required to be accident resistant. During the certification process by the NRC the cask designer must demonstrate, among other things, that the cask would survive a free fall from a height of nine meters impacting onto a flat essentially unyielding target in the orientation that is most likely to damage the cask (10 CFR 71.73). The high standards and conservative approaches required by the NRC for this demonstration include the use of minimum material properties, allowing only small amounts of yielding, and requiring materials with high ductility. These approaches ensure that the casks will not only survive a nine-meter drop, but will also survive much higher speed impacts. In addition to the conservative designs assured by the certification process, there are two additional aspects of the nine-meter drop that provide safety when compared to actual accidents. The first of these is the requirement that the impact be onto an essentially unyielding target. This implies that all of the kinetic energy of the impact will be absorbed by the cask and none by the target. For impacts onto real surfaces, the kinetic energy is absorbed by both the cask and the target. The second aspect is the requirement that the vertical impact is onto a horizontal target. This requirement assures that at some point during the impact the velocity of the cask will be zero, and all of the kinetic energy is converted into strain energy (absorbed by the cask). Most real accidents occur at an angle, and the kinetic energy of the cask is absorbed by multiple impacts instead of all in one impact. In this chapter, all three of these factors will be discussed.

3.2 Finite Element Analyses of Casks

Previous risk studies have been carried out using generic casks. In the case of the Modal Study (Fischer et al, 1987) it was assumed any accident that was more severe than the regulatory hypothetical impact accident would lead to a release from the cask. In NUREG/CR-6672 (Sprung et al., 2000) the impact limiters of the generic casks were assumed to be unable to absorb more energy than the amount from the regulatory hypothetical impact accident (a nine-meter free fall onto an essentially rigid target). Modeling limitations at the time of the studies required both of these assumptions. In reality, casks and impact limiters each have excess capacity to resist impacts. In this study, three NRC certified casks were used instead of generic casks, and the actual excess capacity of those cask designs was included in the analyses.

The response to impacts of 48, 97,145, and 193 kilometers per hour (kph)—equal to 30, 60, 90, and 120 mph— onto an unyielding target in the end, corner, and side orientations for the Rail-Steel and Rail-Pb spent fuel transportation casks were determined using the non-linear transient dynamics explicit finite element code PRESTO (SIERRA, 2009). PRESTO is a Lagrangian code, using a mesh that follows the deformation to analyze solids subjected to large, suddenly applied loads. The code is designed for a massively parallel computing environment and for problems with large deformations, nonlinear material behavior, and contact. Presto has a versatile element library that incorporates both continuum elements and structural elements, such as beams and shells.

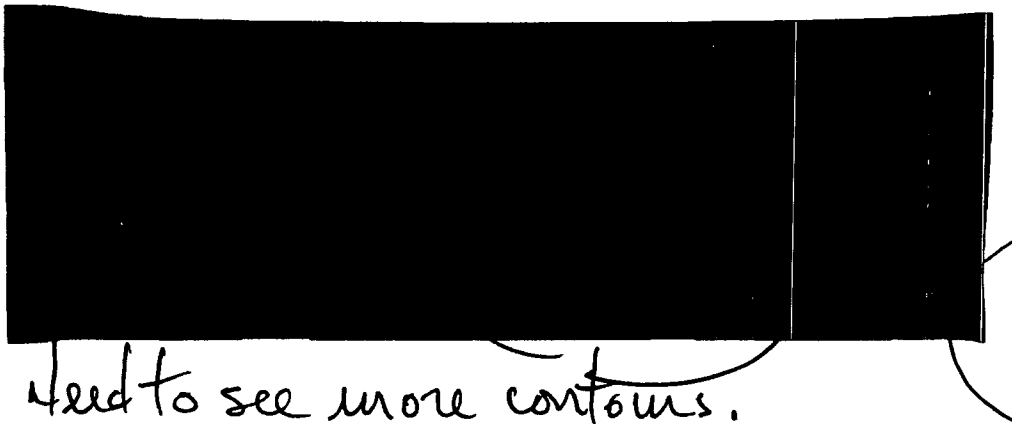

Figure 3-5. Plastic strain in the welded canister of the Rail-Steel for the 193 kph side impact case

Change scale from 0 to Max i.e. 0.7.

3.2.2 Rail-Pb Cask

Finite Element Model

Figure 3-6 shows the overall finite element model of the Rail-Pb cask. This cask uses lead for its gamma-shielding material and transports either 26 directly loaded PWR assemblies or 24 PWR assemblies in a welded multi-purpose canister. The impact limiters on each end of the cask are designed to absorb the kinetic energy of the cask during the regulatory hypothetical impact accident. They are made up of redwood and balsa wood energy absorbing material and a stainless steel skin. Figure 3-7 shows the finite element mesh of the closure end impact limiter (the impact limiter on the other end of the cask is identical). The cask has a dual lid system. The inner lid is attached with 42 1-1/2 inch diameter bolts and sealed with dual o-rings that are elastomeric if the cask is used only for transportation and metallic if the cask is used for storage before transportation case. The outer lid is attached with 36 1-inch diameter bolts and sealed with a single o-ring that is elastomeric if the cask is used only for transportation and metallic if the cask is used for storage before transportation case . Figure 3-8 shows the finite element mesh of the closure bolts and the level of mesh refinement included in these important parts. Details of the finite element models are included in Appendix III.

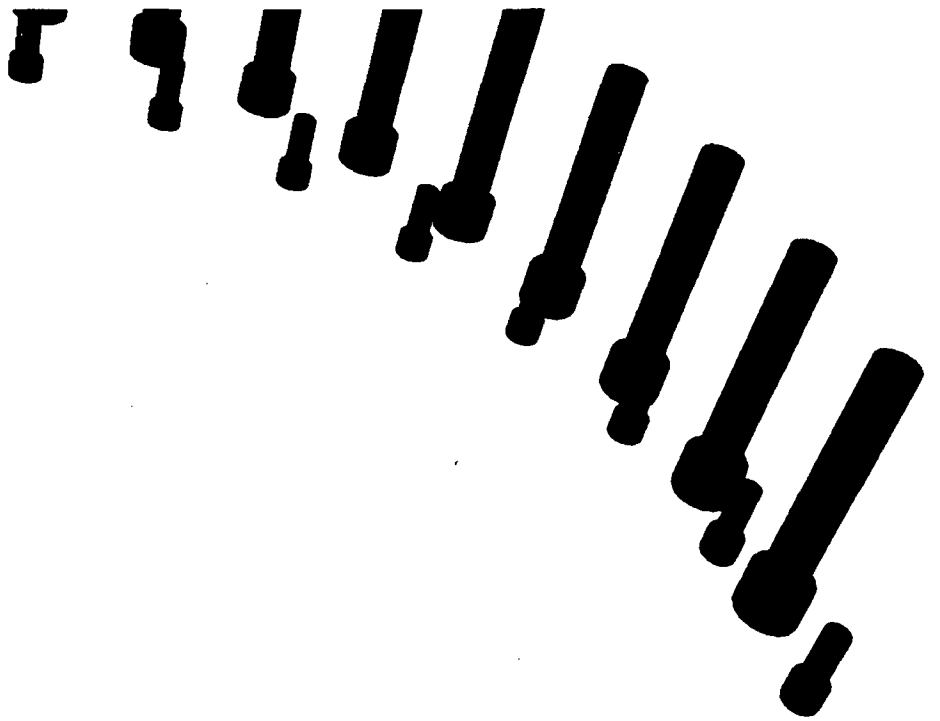

Figure 3-8. Finite element mesh of the Rail-Pb closure bolts for both the inner and outer lids. The longer bolts are for the inner lid and the shorter ones for the outer lid.

Analysis results

For the 48 kph impact analyses (the impact velocity from the regulatory hypothetical impact accident) the impact limiter absorbed almost all of the kinetic energy of the cask and there was no damage to the cask body. The response of the Rail-Pb cask is more complicated than that of the Rail-Steel cask. For the end orientation, as the impact velocity increases, there is first additional damage to the impact limiter because it is absorbing more kinetic energy (this shows the margin of safety in the impact limiter design). At 97 kph there is no significant damage to the cask body or canister. At an impact speed of 145 kph damage to the cask and canister appears to begin. The impact limiter has absorbed all the kinetic energy it can and any additional kinetic energy is absorbed by plastic deformation in the cask body. At this speed there is significant slumping of the lead gamma shielding material, resulting in a loss of shielding near the end of the cask away from the impact point (this is discussed in Chapter 5 and Appendix V). As the impact velocity is increased to 193 kph, the lead slump becomes more pronounced and there is enough plasticity in the lids and closure bolts to result in a loss of sealing capability. For the directly loaded cask (without a welded multi-purpose canister) there could be some loss of radioactive contents if the cask has metallic seals but not for the case with elastomeric seals. A more detailed discussion of leakage is provided later in this section. Figure 3-9 shows the deformed shape of the Rail-Pb following the 193 kph impact in the end-on orientation. The amount of lead slump from this impact is 35.5 cm, and the area without lead shielding is visible in Figure 3-9. Table 3-1 gives the amount of lead slump in each of the analysis cases.

Table 3-4. Deformation of the closure region of the steel-DU-steel truck cask from NUREG/CR-6672, in mm

Cask	Analysis Velocity	Corner Impact		End Impact		Side Impact	
		Opening	Sliding	Opening	Sliding	Opening	Sliding
Steel-DU-Steel Truck	48 kph	0.508	1.778	0.127-0.305	0.025-0.127	0.254	0.508
	97 kph	2.032	1.778	0.254-0.508	0.076-0.152	0.254	0.254
	145 kph	0.508	2.540	-	-	0.254	0.508
	193 kph	0.762	3.810	0.330	0.762	0.102	0.508

3.3 Impacts onto Yielding Targets

All of the analysis results discussed in Section 3.2 were for impacts onto an unyielding essentially rigid target. All real impact accidents involve targets that are to some extent yielding. When a cask impacts a real target the amount of the impact energy that is absorbed by the target and the amount that is absorbed by the cask depend on the relative strength and stiffness of the two objects. For an impact onto a real target to produce the same amount of damage as the impact onto an unyielding target, the force applied to the cask has to be the same. If the target is not capable of sustaining that level of force, it cannot produce the corresponding level of damage in the cask. For the Rail-Pb cask (the only one of the three investigated in this study that has any release) the peak force associated with each of the impact analyses performed is given in **Error! Reference source not found.** ~~Table 3-18~~. In this table the cases that have non-zero hole sizes from Table 3-5 have bold text. It can be seen, that in order to produce sufficient damage for the cask to release any material, the yielding target has to be able to apply a force to the cask greater than 146 MN (33 million pounds). Very few real targets are capable of applying this amount of force.

If the cask hits a flat target, such as the ground, roadway, or railway, it will penetrate into the surface. The greater the penetration depth, the more force the target can exert on the cask. Figure 3-13 shows the relationship between penetration depth and force for the Rail-Pb cask impacting onto hard desert soil. As the cask penetrates the surface, some of its kinetic energy is absorbed by the surface. The amount of energy absorbed by the target is equal to the area underneath the force vs. penetration curve of Figure 3-13. As an example, the end impact at 97 kph onto an unyielding target requires a contact force of 123.9 MN. A penetration depth of approximately 2.2 meters will cause the soil to exert this amount of force. The soil absorbs 142 MJ of energy in being penetrated this distance. Adding the energy absorbed by the soil to the 41 MJ of energy absorbed by the cask gives a total absorbed energy of 183 MJ. For the cask to have this amount of kinetic energy it would have to be traveling at 205 kph. Therefore, a 205 kph impact onto hard desert soil causes the same amount of damage as a 97 kph impact onto an unyielding target. A similar calculation can be performed for other impact speeds, orientations and target types. Table 3-6 provides the resulting equivalent velocities. Where the calculated velocity is more than 250 kph the value in the table is listed as greater than 250. No accident velocities are more than this. The concrete target used is a 23 cm thick slab on engineered fill. This is typical of many concrete roadways and concrete retaining walls adjacent to highways. Details on the calculation of equivalent velocities are included in Appendix III.

This should be stated the other way around.
"The more force, the greater the penetration depth."

using an analysis of a tensile test specimen, and defining failure approximately midway between maximum stress and the final stress. The conservative value was chosen to compensate for the relatively coarse mesh in the bolt.

? If max. strain is 2.13. then the uniform strain is close to 1.0. This seems very light!

Criterion is element value of eqps $\geq$ 1.5

Failure of the inner lid bolts was defined according to Presto convention when a maximum value of eqps was reached in SB-637 Grade N07718 Nickel Alloy Steel.

Criterion is element value of eqps > 0.1

III.2.5 Analysis Results

The deformed shape of the cask following each impact analysis is presented below.

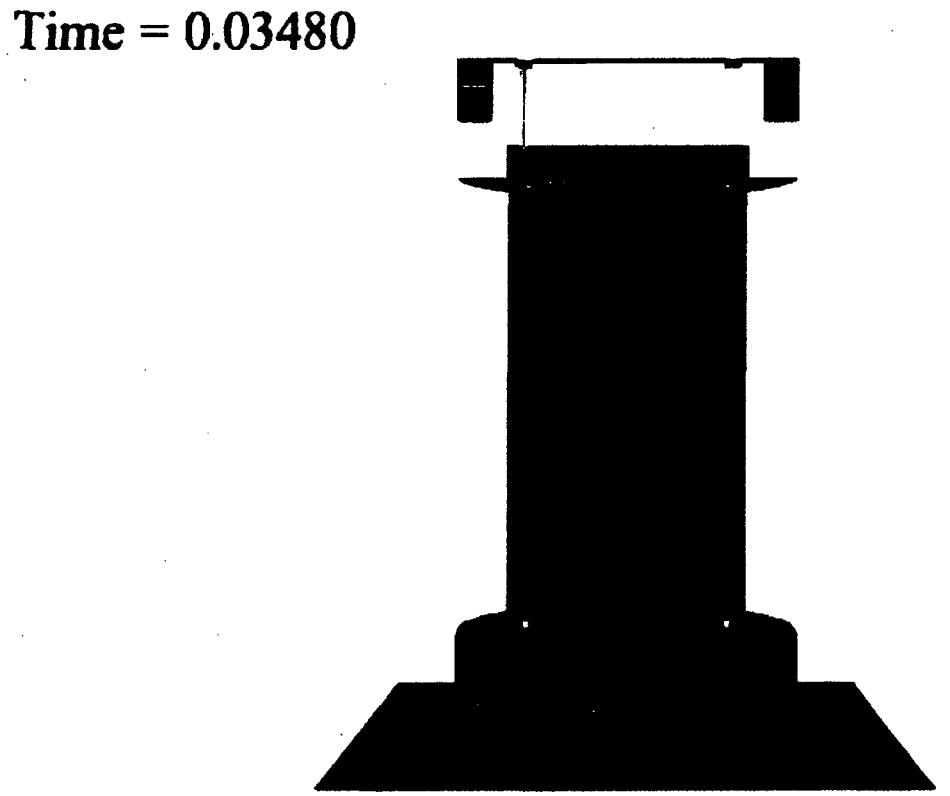

Figure III-28. NAC-STC end impact at 48 KPH (30 MPH)

Table III-1. Available areas for leakage from the NAC-STC cask

Orientation	Speed (KPH)	Location	Lid Gap (mm)	Seal Type	Hole Size (mm²)
End	48	Inner	0.226	Metal	none
		Outer	0	Elastomer	none
	97	Inner	0.056	Metal	none
		Outer	0.003	Elastomer	none
	145	Inner	2.311	Metal	none
		Outer	0.047	Elastomer	none
	193	Inner	5.588	Metal	8796
		Outer	1.829	Elastomer	none
Corner	48	Inner	0.094	Metal	none
		Outer	0.089	Elastomer	none
	97	Inner	0.559	Metal	65
		Outer	0.381	Elastomer	none
	145	Inner	0.980	Metal	599
		Outer	1.448	Elastomer	none
	193	Inner	2.464	Metal	1716
		Outer	1.803	Elastomer	none
Side	48	Inner	0.245	Metal	none
		Outer	0.191	Elastomer	none
	97	Inner	0.914	Metal	799
		Outer	1.600	Elastomer	none
	145	Inner	8*	Metal	>10000
		Outer	25*	Elastomer	>10000
	193	Inner	15*	Metal	>10000
		Outer	50*	Elastomer	>10000

III.2.7 Acknowledgements

Jim Bean at Sandia contributed significantly to the development of this model.

III.3 Impacts onto Yielding Targets

III.3.1 Introduction

The finite element results discussed in the previous section are all for impacts onto a rigid target. For this type of impact, the entire kinetic energy of the impact is absorbed by the cask. For finite element analyses a rigid target is easily implemented by enforcing a no displacement boundary condition at the target surface. In real life, the construction of a rigid target is impossible, but it is possible to construct a target that is sufficiently rigid that increasing its rigidity does not increase the amount of damage to the cask. This is because in real impacts there is a sharing of energy absorption between the cask and the target. If the target is much weaker than the cask, the target will absorb most of the energy. If the target is much stronger than the cask, most of the energy will be absorbed by the cask. In this section the partitioning of the drop energy between the four generic casks and several "real-world" targets will be developed in order to obtain

III.4.2 Description and Method

A typical PWR fuel assembly is shown in Figure III-56. The assembly consists of a series of fuel pins, or rods, grouped together in a square array. The fuels rods are held in place by a series of equally spaced grids. Within the array of fuel tubes are a series of guide tubes in which control rods are place for controlling the fission reaction during operation. The guide tubes are attached to endplates, nozzles or end fittings, which provide rigidity for handling.

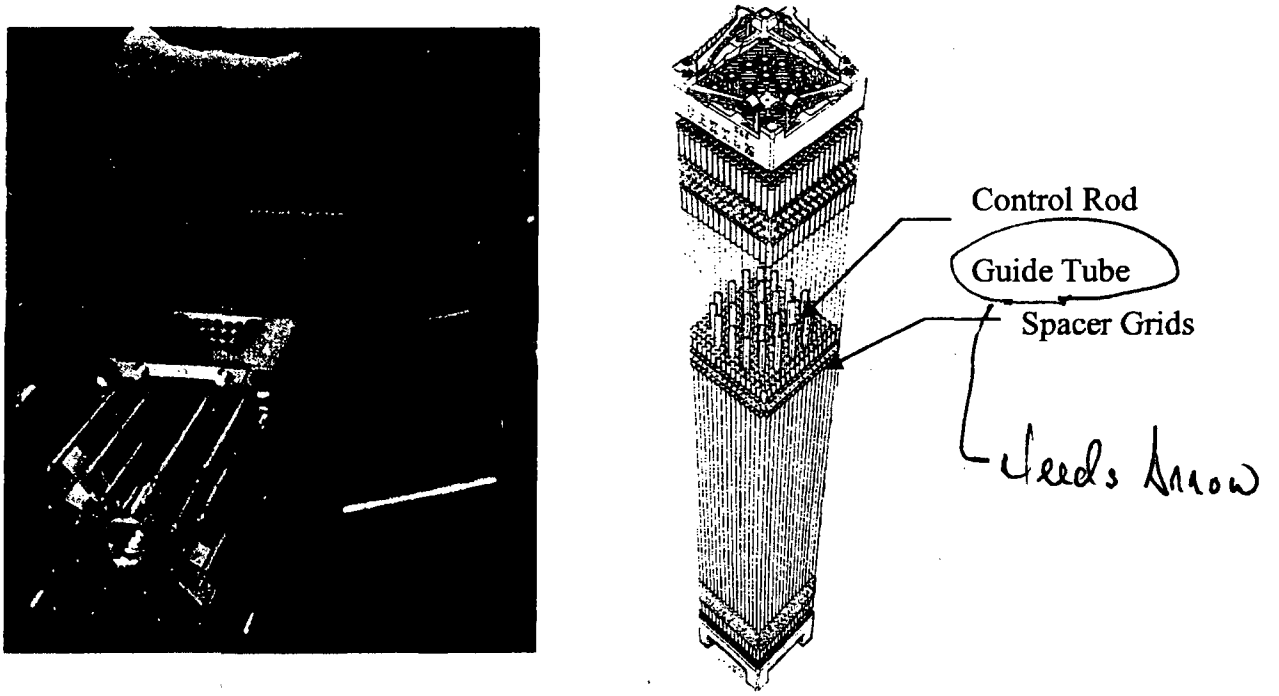

Figure III-56. PWR fuel assembly

An individual fuel rod is shown schematically in Figure #. It is constructed by stacking a series of Uranium Dioxide (UO_2) pellets inside a Zirconium tube, placing a spring on the top of the pellet stack and welding on end caps. A plenum is added at the top of the assembly to provide a sufficient volume to collect released fission gases.

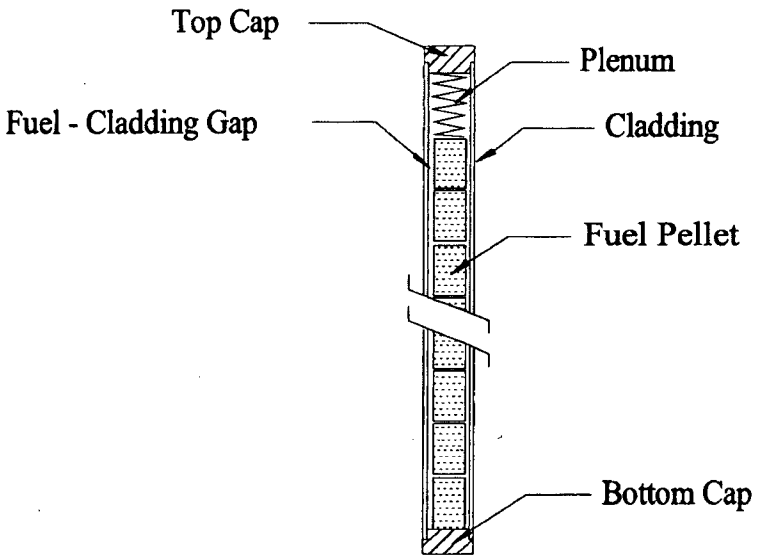

Figure III-57. Fuel rod schematic drawing

The working environment of a reactor is extremely harsh. The fuel rods are subjected to neutron radiation, large thermal gradients, large stress due to external water pressure and large local stress from contact between the pellet and the cladding. Upon the first power cycle, the uranium pellet cracks into pie shaped pieces due to the large radial temperature gradients across the pellet. Over a short period of time (months), the pellets shrink as fine porosity in the fuel is removed by radiation densifications. The cladding slowly creeps down onto the pellet due to its high operating temperature and the external pressure of the coolant. The pellet also begins to expand due to fission product swelling. Over a period of 1-2 years the initial gap between the fuel rod and the pellet is eliminated. However, the contact between the cladding and the fuel pellet in not necessarily circular and uniform. This leads to local increases in the cladding stress. In addition, zirconium is one of the few elements that react with both oxygen and hydrogen. This can lead to a reaction between the ZrO_2 layers on the inner cladding surface and the fuel pellet to form a bonding interface of $(U,Zr)O_2$ between the fuel pellet and the cladding. In essence, bonding the pellet to the cladding wall. In addition, hydride precipitants can also form in the Zircaloy cladding wall.

Upon the removal from the reactor, the state of the spent fuel assembly at any future time depends on the spent fuel's environmental history as well as its condition upon removal from the reactor. The internal gas pressure in a fuel rod having been removed from the reactor now provides a tensile hoop stress on the cladding. This stress along with changes in cladding temperature may allow hydrogen to precipitate out and possibly reform along the circumferential directions (direction of highest stress). Plastic creep in the cladding may cause a gap to develop between the cladding and the fuel pellet and the development of void spaces in the crack pellets. The current material conditions and stress state of any particular rod at the time of an accident is complex and unknown. Therefore, the current material properties and geometric configuration

and axial

From the kinetic energy plots in Figure III-59, it is clear that there is a problem with the beam contact algorithms in LS-DYNA. For the case using the Automatic Single Surface algorithm, the kinetic energy spikes from the initial value of 200 in-lbs to a value of 1000 in-lbs, which is beyond the range shown in the graph. For the LS-DYNA model using the Contact Automatic General algorithm, which was recommended for beam and shell contact by an LS-DYNA instructor, the kinetic energy initially decreases but then spikes beyond the original value of 200 in-lbs to other very large values several times later. For this reason, the LS-DYNA code was not used to model the fuel assembly.

Initially, the Abaqus/Explicit code using the General Contact algorithm looked much better. The kinetic energy plot for the test model indicated an initial drop with a small rebound and a final tapering off. However, further analyses of the same model with different numbers of elements also showed a spike in kinetic energy. These results are presented in Figure III-60. For the model containing six elements along the beam length, there is a huge rebound in the kinetic energy to over 3000 in-lbs. Consultation with Abaqus personnel resulted in them finding a bug in the code and sending out a new version of their code to Sandia.

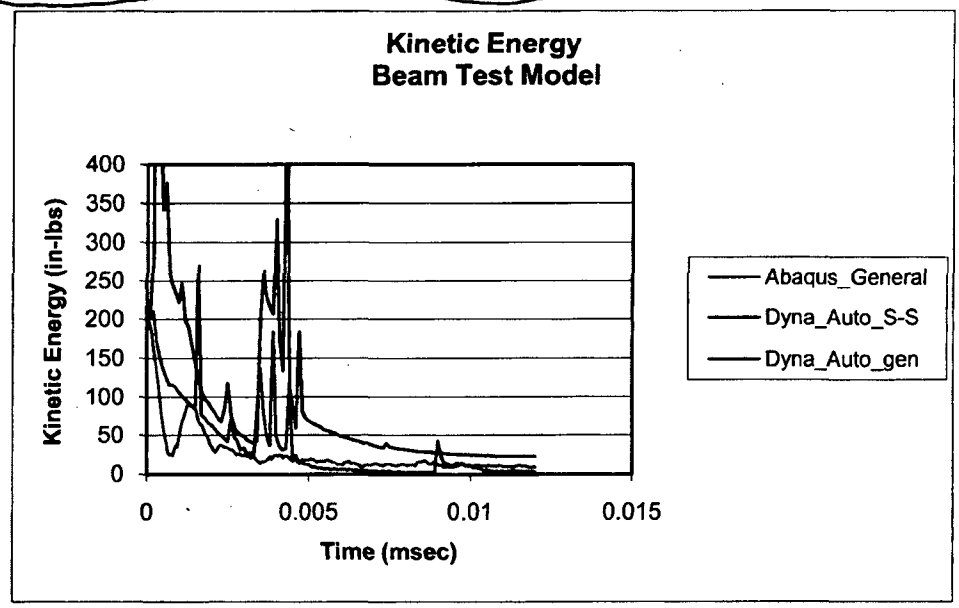

Figure III-59 Kinetic energy for code test models

This should NOT be discussed in the NUREG.

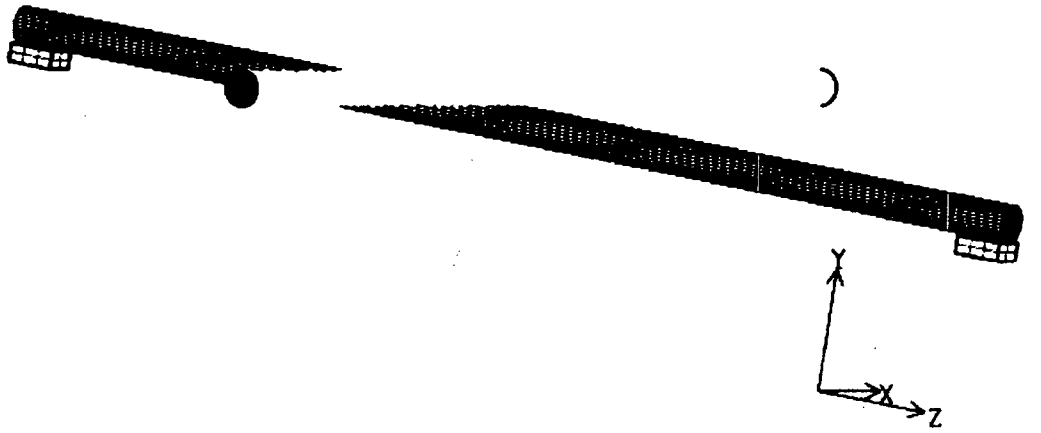

Figure III-65. Hexahedron test model for solid rod–to-rod contact in Abaqus/Explicit

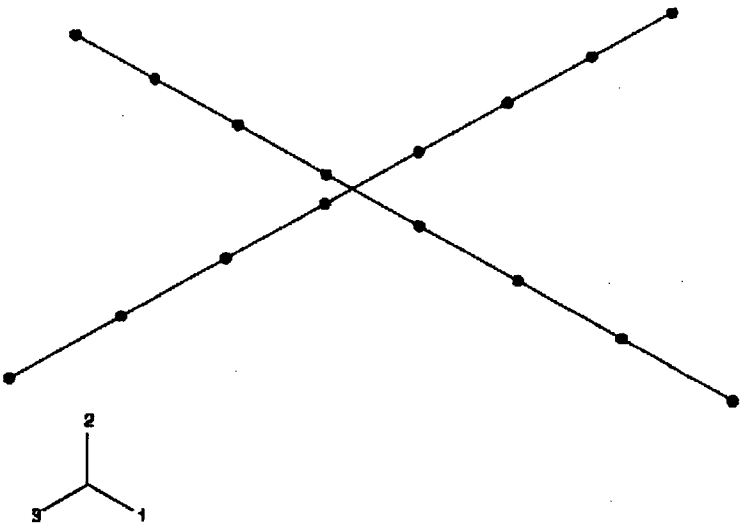

Figure III-66. Test model for beam-to-beam contact in Abaqus/Explicit

The results from the two finite element rod models are shown in Figure III-67 and Figure III-68. For the same mass, impact velocity and cross-sectional geometry, the two models generate two different sets of contact forces. As shown in Figure III-67, the beam element impact forces are much large and shorter in duration than those generated from the hex rod model. The magnitudes of the forces differ by about a factor of five. An additional check was made comparing the hexahedron Abaqus/Explicit model to a similar model run in the Sandia code PRONTO3D. Both codes generated similar contact and reaction forces. Therefore, it is presumed that the beam element contact algorithm in Abaqus/Explicit is in error. Abaqus personnel were contacted and they are investigating the problem, but no resolution has been reached. Continued evaluation of the two models generated the curves shown in Figure III-68. For the velocity range of interest there is a good linear fit for each curve. Therefore, in transferring the loads between the beam